

Cerberus: A MOOSE-based application for solving the SP_3 equations

ANS Annual Meeting 2021

Roberto Fairhurst Agosta, Kathryn D. Huff

Advanced Reactors and Fuel Cycles
University of Illinois at Urbana-Champaign

June 14, 2021



ILLINOIS

Outline

1 Introduction

Objectives
Motivation

2 Methodology

Equations
Implementation
Kernels

3 Results

1-G, 2-D
2-G, 2-D
2-G, 3-D

4 Final Remarks

Conclusions
Acknowledgement
Questions



Objectives

- Describe the implementation of the SP_3 equations in a MOOSE-based application.
- Verify the implementation by conducting the following exercises:
 - One-group, two-dimensional eigenvalue problem.
 - C5 MOX Benchmark (2D)
 - C5 MOX Benchmark (3D mini-core variation)



Motivation

Why a neutronics solver?

- Neutronics provide information on the power distribution.
- Crucial role in the thermal-fluids behavior of a reactor.
- Multi-physics simulations for safety assessment.

Why the SP_3 equations?

- Fewer equations than P_3 .
- Reduces the computational expense.
- Conserves a reasonable accuracy.
- More accurate solution than diffusion approximation.

Why MOOSE?

- Partial differential equations describe the reactor physics.
- Computational framework for solving coupled equation systems.
- Open-source, enabling wider collaboration.
- API that facilitates coupling between various applications targeting different phenomena.

Outline

① Introduction

Objectives

Motivation

② Methodology

Equations

Implementation

Kernels

③ Results

1-G, 2-D

2-G, 2-D

2-G, 3-D

④ Final Remarks

Conclusions

Acknowledgement

Questions

P_3 equations

- P_N expands the angular dependence in spherical harmonics.
- For $N=3$, steady-state, and one-dimension [5]:

$$\frac{d}{dx}\phi_{1,g} + \Sigma_{t,g}\phi_{0,g} = \sum_{g'=1}^G \Sigma_{s0,g' \rightarrow g}\phi_{0,g'} + \frac{\chi_g}{k_{eff}} \sum_{g'=1}^G \nu \Sigma_{f,g'}\phi_{0,g'} + Q_{0,g} \quad (1)$$

$$\frac{1}{3} \frac{d}{dx}\phi_{0,g} + \frac{2}{3} \frac{d}{dx}\phi_{2,g} + \Sigma_{t,g}\phi_{1,g} = \sum_{g'=1}^G \Sigma_{s1,g' \rightarrow g}\phi_{1,g'} + Q_{1,g} \quad (2)$$

$$\frac{2}{5} \frac{d}{dx}\phi_{1,g} + \frac{3}{5} \frac{d}{dx}\phi_{3,g} + \Sigma_{t,g}\phi_{2,g} = \sum_{g'=1}^G \Sigma_{s2,g' \rightarrow g}\phi_{2,g'} + Q_{2,g} \quad (3)$$

$$\frac{3}{7} \frac{d}{dx}\phi_{2,g} + \Sigma_{t,g}\phi_{3,g} = \sum_{g'=1}^G \Sigma_{s3,g' \rightarrow g}\phi_{3,g'} + Q_{3,g}. \quad (4)$$

P_3 equations (2)

Assumptions [2]:

- isotropic external source
- negligible anisotropic group-to-group scattering

$$\frac{d}{dx}\phi_{1,g} + \Sigma_{0,g}\phi_{0,g} = \sum_{g' \neq g}^G \Sigma_{s0,g' \rightarrow g}\phi_{0,g'} + \frac{\chi_g}{k_{eff}} \sum_{g'=1}^G \nu \Sigma_{f,g'}\phi_{0,g'} + Q_{0,g} \quad (5)$$

$$\frac{1}{3} \frac{d}{dx}\phi_{0,g} + \frac{2}{3} \frac{d}{dx}\phi_{2,g} + \Sigma_{1,g}\phi_{1,g} = 0 \quad (6)$$

$$\frac{2}{5} \frac{d}{dx}\phi_{1,g} + \frac{3}{5} \frac{d}{dx}\phi_{3,g} + \Sigma_{2,g}\phi_{2,g} = 0 \quad (7)$$

$$\frac{3}{7} \frac{d}{dx}\phi_{2,g} + \Sigma_{3,g}\phi_{3,g} = 0. \quad (8)$$

P_3 equations (3)

With the following definitions:

$$D_{0,g} = \frac{1}{3\Sigma_{1,g}}, \quad D_{2,g} = \frac{9}{35\Sigma_{3,g}}$$

$$\Phi_{0,g} = \phi_{0,g} + 2\phi_{2,g}, \quad \Phi_{2,g} = \phi_{2,g}$$

the equations become:

$$-D_{0,g} \frac{d^2}{dx^2} \Phi_{0,g} + \Sigma_{0,g} \Phi_{0,g} - 2\Sigma_{0,g} \Phi_{2,g} = S_{0,g} \quad (9)$$

$$-D_{2,g} \frac{d^2}{dx^2} \Phi_{2,g} + \left(\Sigma_{2,g} + \frac{4}{5} \Sigma_{0,g} \right) \Phi_{2,g} - \frac{2}{5} \Sigma_{0,g} \Phi_{0,g} = -\frac{2}{5} S_{0,g} \quad (10)$$

where

$$S_{0,g} = \sum_{g' \neq g}^G \Sigma_{s0,g' \rightarrow g} (\Phi_{0,g'} - 2\Phi_{2,g'}) + \frac{\chi_g}{k_{\text{eff}}} \sum_{g'=1}^G \nu \Sigma_{f,g'} (\Phi_{0,g'} - 2\Phi_{2,g'}) + Q_{0,g}.$$

SP_3 approximation

- P_N : yields the exact transport solution as $N \rightarrow \infty$.
- 3D: $(N + 1)^2$ equations. If $N = 3$, 16 equations.
- 1D: $(N + 1)$ equations yield $(N + 1)/2$. If $N = 3$, 2 equations.
- SP_N approximation replaces $\frac{d^2}{dx^2}$ by Δ .

SP_3 equations

$$-D_{0,g}\Delta\Phi_{0,g} + \Sigma_{0,g}\Phi_{0,g} - 2\Sigma_{0,g}\Phi_{2,g} = S_{0,g} \quad (11)$$

$$-D_{2,g}\Delta\Phi_{2,g} + \left(\Sigma_{2,g} + \frac{4}{5}\Sigma_{0,g}\right)\Phi_{2,g} - \frac{2}{5}\Sigma_{0,g}\Phi_{0,g} = -\frac{2}{5}S_{0,g}. \quad (12)$$

With the Marshak vacuum BCs [1]

$$\frac{1}{4}\Phi_{0,g} \pm \frac{1}{2}\hat{n} \cdot J_{0,g} - \frac{3}{16}\Phi_{2,g} = 0 \quad (13)$$

$$-\frac{3}{80}\Phi_{0,g} \pm \frac{1}{2}\hat{n} \cdot J_{2,g} + \frac{21}{80}\Phi_{2,g} = 0 \quad (14)$$

where

$$J_{n,g} = -D_{n,g}\nabla\Phi_{n,g}.$$

MOOSE



- Computational framework for solving coupled equation systems.
- Input are the weak form of the equations.
- MOOSE and LibMesh translate them into residual and Jacobian functions.
- Petsc solution routines solve the equations.

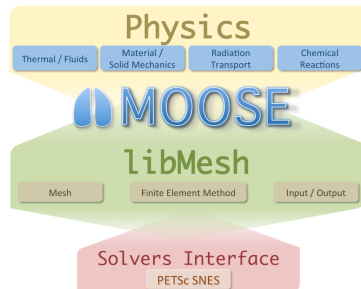


Figure: MOOSE framework. Image reproduced from [6].

Weak form



Example Code

Strong Form

$$\rho C_p \frac{\partial T}{\partial t} - \nabla \cdot k(T, B) \nabla T = f$$

Weak Form

$$\int_{\Omega} \rho C_p \frac{\partial T}{\partial t} \psi_i + \int_{\Omega} k \nabla T \cdot \nabla \psi_i - \int_{\partial \Omega} k \nabla T \cdot \mathbf{n} \psi_i - \int_{\Omega} f \psi_i = 0$$

Kernel Kernel BoundaryCondition Kernel

Actual Code

```
return _k[_qp]*_grad_u[_qp]*_grad_test[_i][_qp];
```

Figure: Translation into MOOSE kernels procedure [6].

Weak form: Equation 1

$$\begin{aligned}
& \langle D_{0,g} \nabla \Phi_{0,g}, \nabla \Psi \rangle - \langle D_{0,g} \nabla \Phi_{0,g}, \Psi \rangle_{BC} + \langle \Sigma_{0,g} \Phi_{0,g}, \Psi \rangle + \langle -2\Sigma_{0,g} \Phi_{2,g}, \Psi \rangle \\
& + \left\langle - \sum_{\substack{g'=1 \\ g' \neq g}}^G \Sigma_{s0,g' \rightarrow g} (\Phi_{0,g'} - 2\Phi_{2,g'}), \Psi \right\rangle \\
& + \left\langle - \frac{\chi_g}{k_{eff}} \sum_{g'=1}^G \nu \Sigma_{f,g'} (\Phi_{0,g'} - 2\Phi_{2,g'}), \Psi \right\rangle + \langle -Q_{0,g}, \Psi \rangle = 0
\end{aligned} \tag{15}$$

with the boundary condition

$$\langle D_{0,g} \nabla \Phi_{0,g}, \Psi \rangle_{BC} = \left\langle \frac{1}{2} \Phi_{0,g} - \frac{3}{4} \Phi_{2,g}, \Psi \right\rangle_{BC}. \tag{16}$$

Weak form: Equation 2

$$\begin{aligned}
& \langle D_{2,g} \nabla \Phi_{2,g}, \nabla \Psi \rangle - \langle D_{2,g} \nabla \Phi_{2,g}, \Psi \rangle_{BC} + \left\langle \left(\Sigma_{2,g} + \frac{4}{5} \Sigma_{0,g} \right) \Phi_{2,g}, \Psi \right\rangle \\
& + \left\langle -\frac{2}{5} \Sigma_{0,g} \Phi_{0,g}, \Psi \right\rangle + \left\langle \frac{2}{5} \sum_{g' \neq g}^G \Sigma_{s0,g' \rightarrow g} (\Phi_{0,g'} - 2\Phi_{2,g'}), \Psi \right\rangle \\
& + \left\langle \frac{2}{5} \frac{\chi_g}{k_{eff}} \sum_{g'=1}^G \nu \Sigma_{f,g'} (\Phi_{0,g'} - 2\Phi_{2,g'}), \Psi \right\rangle + \left\langle \frac{2}{5} Q_{0,g}, \Psi \right\rangle = 0. \quad (17)
\end{aligned}$$

with the boundary condition

$$\langle D_{2,g} \nabla \Phi_{2,g}, \Psi \rangle_{BC} = \left\langle -\frac{3}{40} \Phi_{0,g} + \frac{21}{40} \Phi_{2,g}, \Psi \right\rangle_{BC}. \quad (18)$$

Cerberus Kernels: Equation 1

Table: SP_3 kernels.

Kernel name	Equation 1
SP3Diffusion	$\langle D_{0,g} \nabla \Phi_{0,g}, \nabla \Psi \rangle$
SP3SigmaR	$\langle \Sigma_{0,g} \Phi_{0,g}, \Psi \rangle$
SP3SigmaCoupled	$\langle -2\Sigma_{0,g} \Phi_{2,g}, \Psi \rangle$
SP3InScatter	$\langle -\sum_{g' \neq g}^G \Sigma_{s0,g' \rightarrow g} (\Phi_{0,g'} - 2\Phi_{2,g'}), \Psi \rangle$
SP3FissionEigenKernel	$\langle -\frac{\chi_g}{k_{eff}} \sum_{g'=1}^G \nu \Sigma_{f,g'} (\Phi_{0,g'} - 2\Phi_{2,g'}), \Psi \rangle$
BodyForce (MOOSE)	$\langle -Q_{0,g}, \Psi \rangle$
BC Kernel name	
SP3Vacuum	$\langle \frac{1}{2} \Phi_{0,g} - \frac{3}{4} \Phi_{2,g}, \Psi \rangle_{BC}$

Cerberus Kernels: Equation 2

Table: SP_3 kernels.

Kernel name	Equation 2
SP3Diffusion	$\langle D_{2,g} \nabla \Phi_{2,g}, \nabla \Psi \rangle$
SP3SigmaR	$\langle (\Sigma_{2,g} + \frac{4}{5} \Sigma_{0,g}) \Phi_{2,g}, \Psi \rangle$
SP3SigmaCoupled	$\langle -\frac{2}{5} \Sigma_{0,g} \Phi_{0,g}, \Psi \rangle$
SP3InScatter	$\langle \frac{2}{5} \sum_{g' \neq g}^G \Sigma_{s0,g' \rightarrow g} (\Phi_{0,g'} - 2\Phi_{2,g'}), \Psi \rangle$
SP3FissionEigenKernel	$\langle \frac{2}{5} \frac{\chi_g}{k_{eff}} \sum_{g'=1}^G \nu \Sigma_{f,g'} (\Phi_{0,g'} - 2\Phi_{2,g'}), \Psi \rangle$
BodyForce (MOOSE)	$\langle \frac{2}{5} Q_{0,g}, \Psi \rangle$
BC Kernel name	
SP3Vacuum	$\langle -\frac{3}{40} \Phi_{0,g} + \frac{21}{40} \Phi_{2,g}, \Psi \rangle_{BC}$

Outline

1 Introduction

Objectives
Motivation

2 Methodology

Equations
Implementation
Kernels

3 Results

1-G, 2-D
2-G, 2-D
2-G, 3-D

4 Final Remarks

Conclusions
Acknowledgement
Questions

One-group, two-dimensional eigenvalue problem

- Problem presented in Brantley and Larsen, 2000 [2].
- One-energy group.
- Two-dimensional problem.
- Two materials: fuel and moderator.

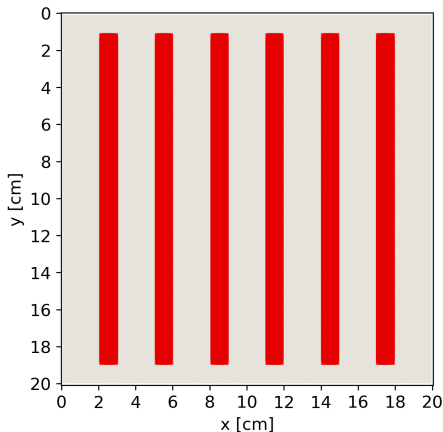


Figure: Problem's geometry.

One-group, two-dimensional eigenvalue problem (2)

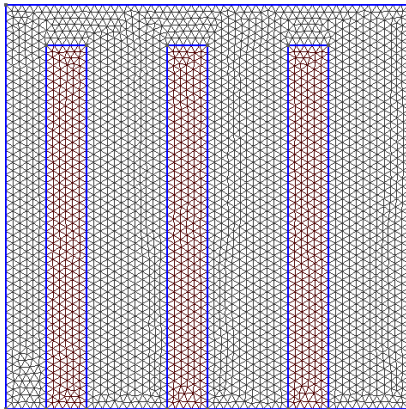


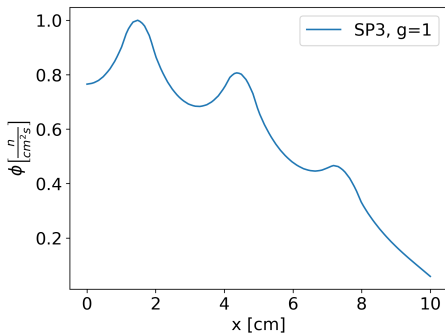
Figure: Gmsh 2D mesh.

One-group, two-dimensional eigenvalue problem (3)



Table: Eigenvalue comparison.

k_{Ref}	k_{SP_3}	Δ_ρ
0.79862	0.79854	12

Figure: Scalar flux over line at $y=4.5$ cm.

C5 MOX Benchmark

- Exercise defined in 1994 by OECD/NEA [4].
- Two-energy groups.
- Two-dimensional problem.
- Two types of fuel: UO_2 , MOX.

C5 MOX Benchmark (2)

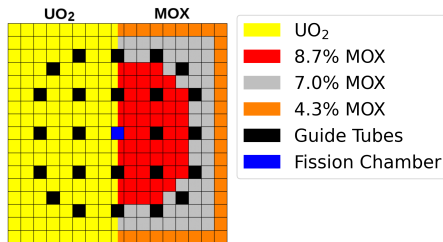
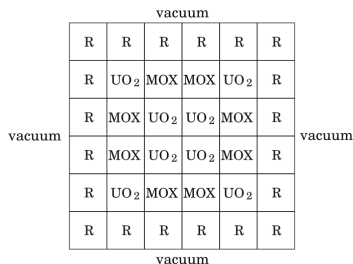


Figure: 2-D C5 MOX benchmark configuration. *R* represents the reflectors. Image reproduced from [3].

Figure: Structure of the UO₂ and MOX assemblies.

C5 MOX Benchmark (3)

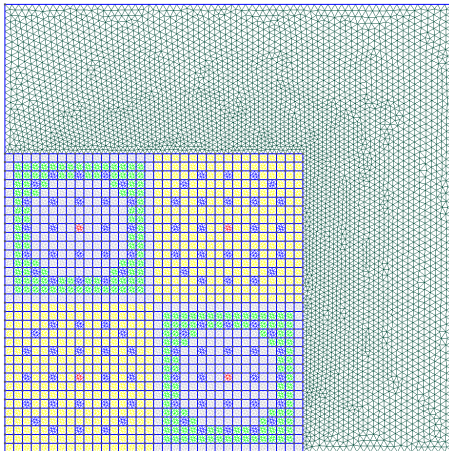


Figure: Gmsh 2D mesh.



C5 MOX Benchmark (4)

If the higher order information of the scattering cross-section is not available (no correction):

$$D_{0,g} = \frac{1}{3\Sigma_{1,g}} = \frac{1}{3\Sigma_{t,g}} \quad (19)$$

The definition of the benchmark [4] recommends applying the diagonal transport correction:

$$D_{0,g} = \frac{1}{3\Sigma_{tr,g}} \quad (20)$$
$$\Sigma_{tr,g} = \Sigma_{t,g} - \bar{\mu}_g \Sigma_{s0,g}$$

where

$\Sigma_{tr,g}$ = group g transport cross-section

$\bar{\mu}_g$ = group g average cosine deviation angle.

C5 MOX Benchmark (5)



	C5G2 Benchmark	Cerberus	
Case	k_{Ref}	k_{SP_3}	Δ_ρ [pcm]
No correction	0.96969	0.97106	145
Transport correction	0.93755	0.93792	43

C5 MOX Benchmark (6)

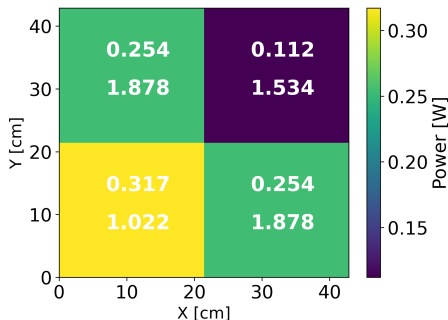


Figure: Assembly power distribution. Top: Assembly power. Bottom: Pin power relative difference expressed in %.

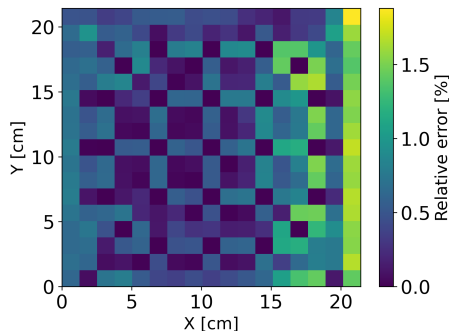


Figure: MOX assembly pin power relative difference expressed in %.

C5 MOX Benchmark (7)

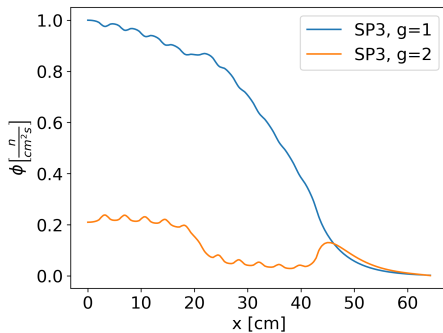


Figure: Scalar flux at $y=10.71\text{cm}$.

C5 MOX 3D



- 3D mini-core variation of the C5 MOX benchmark introduced by Ryu et al., 2013 [7].
- Two-energy group.
- Three-dimensional problem.
- Three materials: UO_2 , MOX, and reflector.

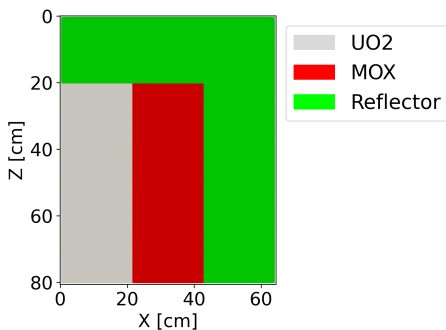


Figure: Axial layout of the C5G2 3D Benchmark.

C5 MOX 3D (2)



Table: Eigenvalue comparison.

k_{Ref}	k_{SP_3}	Δ_ρ
0.91974	0.91979	6

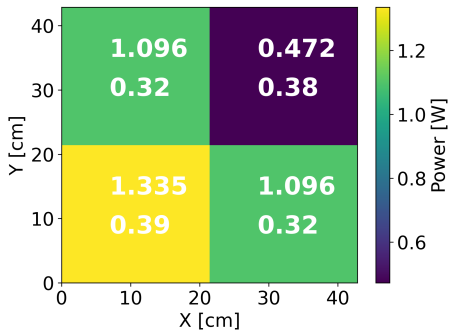


Figure: Power distribution in the C5G2 3D Benchmark. Top: power distribution. Bottom: relative difference expressed in %.



Outline

1 Introduction

Objectives
Motivation

2 Methodology

Equations
Implementation
Kernels

3 Results

1-G, 2-D
2-G, 2-D
2-G, 3-D

4 Final Remarks

Conclusions
Acknowledgement
Questions



Conclusions

- Implemented the kernels to solve the steady-state SP_3 equations in the MOOSE-based application Cerberus.
- Conducted three exercises whose reference results were known:
 - First exercise: Eigenvalue difference of 12 pcm.
 - Second exercise:
 - Eigenvalue difference of 145 pcm.
 - Pin power distribution within 2% difference.
 - Third exercise:
 - Eigenvalue difference of 6 pcm.
 - Assembly power distribution within 1% difference.
- Transport correction is necessary when the scattering higher moments are unknown.
- Future work may develop new applications or integrate this application to other physics solvers.

Acknowledgement



This research was performed using funding received from the DOE Office of Nuclear Energy's University Program (Project 20-19693, DE-NE0008972) 'Evaluation of micro-reactor requirements and performance in an existing well-characterized micro-grid'.

**Thank you.
Questions?**

References I

- [1] C. Beckert and U. Grundmann.
Development and verification of a nodal approach for solving the multigroup P3 equations.
Annals of Nuclear Energy, 2007.
- [2] P.S. Brantley and E.W. Larsen.
The Simplified P3 Approximation.
Nuclear Science and Engineering, 2000.
- [3] M. Capilla, D. Ginestar, and G. Verdú.
Applications of the multidimensional equations to complex fuel assembly problems.
Annals of Nuclear Energy, 36(10):1624–1634, October 2009.
- [4] C. Cavarec, J.F. Perron, D. Verwaerde, and J.P. West.
Benchmark Calculations of Power Distributions within Assemblies.
Technical Report HT-12/94006 A, NEA/NSC/DOC (94) 28, Nuclear Energy Agency Committee on Reactor Physics, 1994.
- [5] B. Davidson.
Neutron Transport Theory.
Oxford University Press, London, 1957.

References II

[6] INL.

Moose Workshop Slides, December 2020.

<https://mooseframework.inl.gov/workshop>.

[7] Eun Hyun Ryu and Han Gyu Joo.

Finite element method solution of the simplified P3 equations for general geometry applications.

Annals of Nuclear Energy, 56:194–207, June 2013.